Brain Structure and Function (2019) 224:811–827
https://doi.org/10.1007/s00429-018-1801-3

ORIGINAL ARTICLE

Granule neuron precursor cell proliferation is regulated by NFIX and intersectin 1 during postnatal cerebellar development

James Fraser[1] · Alexandra Essebier[2] · Alexander S. Brown[5] · Raul Ayala Davila[1] · Ameet S. Sengar[6] · YuShan Tu[6] · Kathleen S. Ensbey[7] · Bryan W. Day[7] · Matthew P. Scott[5] · Richard M. Gronostajski[8] · Brandon J. Wainwright[3] · Mikael Boden[2] · Tracey J. Harvey[1] · Michael Piper[1,4]

Received: 8 March 2018 / Accepted: 24 November 2018 / Published online: 3 December 2018

Abstract

Cerebellar granule neurons are the most numerous neuronal subtype in the central nervous system. Within the developing cerebellum, these neurons are derived from a population of progenitor cells found within the external granule layer of the cerebellar anlage, namely the cerebellar granule neuron precursors (GNPs). The timely proliferation and differentiation of these precursor cells, which, in rodents occurs predominantly in the postnatal period, is tightly controlled to ensure the normal morphogenesis of the cerebellum. Despite this, our understanding of the factors mediating how GNP differentiation is controlled remains limited. Here, we reveal that the transcription factor nuclear factor I X (NFIX) plays an important role in this process. Mice lacking *Nfix* exhibit reduced numbers of GNPs during early postnatal development, but elevated numbers of these cells at postnatal day 15. Moreover, $Nfix^{-/-}$ GNPs exhibit increased proliferation when cultured in vitro, suggestive of a role for NFIX in promoting GNP differentiation. At a mechanistic level, profiling analyses using both ChIP-seq and RNA-seq identified the actin-associated factor *intersectin 1* as a downstream target of NFIX during cerebellar development. In support of this, mice lacking *intersectin 1* also displayed delayed GNP differentiation. Collectively, these findings highlight a key role for NFIX and intersectin 1 in the regulation of cerebellar development.

Keywords NFIX · Cerebellum · External granular layer · Granule neuron

Introduction

During nervous system development, transcription factors play a variety of key roles, including the regulation of the genes that control proliferation and self-renewal, differentiation, migration and maturation. The cerebellum provides a salient example of how different transcription factors

James Fraser and Alexandra Essebier contributed equally to this work.

Electronic supplementary material The online version of this article (https://doi.org/10.1007/s00429-018-1801-3) contains supplementary material, which is available to authorized users.

✉ Tracey J. Harvey
t.harvey1@uq.edu.au

✉ Michael Piper
m.piper@uq.edu.au

1 The School of Biomedical Sciences, The University of Queensland, Brisbane 4072, Australia

2 The School of Chemistry and Molecular Bioscience, The University of Queensland, Brisbane 4072, Australia

3 Institute for Molecular Bioscience, The University of Queensland, Brisbane 4072, Australia

4 Queensland Brain Institute, The University of Queensland, Brisbane 4072, Australia

5 Department of Developmental Biology, Stanford University School of Medicine, Stanford, CA, USA

6 Program in Neurosciences & Mental Health, The Hospital for Sick Children, Toronto M5G 0A8, Canada

7 Cell and Molecular Biology Department, Translational Brain Cancer Research Laboratory, QIMR Berghofer MRI, Brisbane, QLD 4006, Australia

8 Department of Biochemistry, Program in Genetics, Genomics and Bioinformatics, Center of Excellence in Bioinformatics and Life Sciences, State University of New York at Buffalo, Buffalo, NY, USA

mediate the development of neural stem cells and their progeny (Heng et al. 2012; Kilpatrick et al. 2012; Piper et al. 2011). The cerebellum coordinates the timing and execution of motor commands in response to sensory feedback from the peripheral nervous system (Leto et al. 2015; Martinez et al. 2013). In the developing rodent brain, the cerebellum is ultimately derived at approximately embryonic day (E) 12 from precursor cells in the rhombic lip, a rapidly dividing group of neuroepithelial cells located within the emerging hindbrain (Chizhikov and Millen 2003). The specification and proliferation of these cells is driven in large part by transcription factors including OTX2, PAX6 and ATOH1 (Landsberg et al. 2005; Machold and Fishell 2005; Vernay et al. 2005). These progenitor cells then migrate to populate the outer surface of the cerebellar anlage (Miale and Sidman 1961), forming a secondary, transient proliferative zone known as the external granule cell layer (EGL) (Chizhikov and Millen 2003). The proliferation of these cells continues well into the postnatal period, a process regulated by transcription factors including PAX6, ZIC1 and ZIC3 (Aruga 2004; Engelkamp et al. 1999). During the first 2 weeks postnatally, progenitor cells within the EGL differentiate into immature granule neurons, which subsequently migrate radially into the emerging cerebellum to the inner granule layer (IGL), where they fully mature. Again, transcription factors such as NEUROD1, MBH1, MBH2, ZIC1 and ZIC2 contribute to these processes (Aruga et al. 2002; Kawauchi and Saito 2008; Pan et al. 2009).

Another suite of transcription factors that have been shown to regulate development of the hindbrain and cerebellum are the nuclear factor I (NFI) family (Heng et al. 2012; Kilpatrick et al. 2012). These transcription factors are expressed in a variety of progenitor cell populations within the developing (Chaudhry et al. 1997; Piper et al. 2014, 2010) and adult nervous system (Chen et al. 2017; Heng et al. 2015), as well as by progenitor cells in other regions of the body (Chang et al. 2013; Messina et al. 2010; Harris et al. 2015). NFIs have been implicated in a variety of facets of brainstem development (Kilpatrick et al. 2012). NFIB, for example, has been shown to mediate basilar pontine development, as precerebellar neurons and pontine neurons exhibit delayed differentiation in the absence of this gene (Kumbasar et al. 2009). NFIA and NFIB are also expressed by granule neuron progenitors (GNPs) within the postnatal EGL, and by the progeny of these cells as they migrate to, and differentiate within, the postnatal IGL (Wang et al. 2007). Importantly, many aspects of granule neuron migration and maturation are abnormal in *Nfia*$^{-/-}$ mice, including migration, axonal formation and arborisation of dendritic processes (Wang et al. 2007, 2004). NFIs have further been shown to control these processes via the regulation of genes that mediate granule neuron maturation, including *Tag1, Wnt7a* and *Gabra6* (Wang et al. 2004, 2007, 2010). These findings highlight the critical role played by NFI transcription factors in cerebellar development.

We have recently shown that another NFI family member, NFIX, is highly expressed by GNPs within the postnatal EGL (Fraser et al. 2017). Moreover, *Nfix*-deficient mice exhibit delayed cerebellar development (Piper et al. 2011). These findings are suggestive of NFIX mediating progenitor cell differentiation within the postnatal cerebellum. Our previous work within the forebrain supports this concept, as we have shown NFIX to be a pivotal factor in promoting neural stem cell differentiation within the neocortex (Campbell et al. 2008; Heng et al. 2015) and hippocampus (Harris et al. 2016; Heng et al. 2014), via the transcriptional regulation of genes such as *Sox9, Gfap, Insc* and *Bbx* (Dixon et al. 2013; Harris et al. 2016; Heng et al. 2014). Here we sought to define the mechanism by which NFIX regulates GNP biology. We reveal that *Nfix*$^{-/-}$ mice exhibit delayed GNP differentiation in vivo, and that *Nfix*-deficient GNPs proliferate more extensively than control GNPs in vitro. Moreover, we used both chromatin immunoprecipitation and sequencing (ChIP-seq) and RNA sequencing (RNA-seq) to identify potential NFI targets within postnatal GNPs, and identified *intersectin 1* as a target for NFIX-mediated transcriptional activation. Crucially, analysis of *intersectin 1* mutant mice revealed phenotypically similar cerebellar defects. These findings thus provide novel insights into the transcriptional regulation of GNP differentiation, revealing that NFIX-mediated regulation of *intersectin 1* plays a central role in ensuring the timely differentiation of this postnatal neural progenitor cell pool.

Methods

Animals and ethics approvals

This research involved the use of animals. *Nfix*$^{+/+}$ and *Nfix*$^{-/-}$ mice were used in this study with approval from the University of Queensland Animal Ethics Committee (AEC approval numbers: QBI/143/16/NHMRC/ARC and QBI/149/16/ARC). *Itsn1*-deficient animals were also used in accordance with the recommendations of the Canadian Council on Animal Care and animal care regulations and policies of the Hospital for Sick Children, Toronto. Animals were genotyped as previously described (Campbell et al. 2008; Sengar et al. 2013). Primer sequences are available on request. All experiments were performed according to the Australian Code of Practice for the Care and Use of Animals for Scientific Purposes. Pregnant females were produced by placing male and female mice together overnight. The next day, females were inspected for the presence of a vaginal plug and, if present, this day was designated as E0. The day of birth was designated as postnatal day (P) 0. Mice

were housed in Optimice IVC caging, with double HEPA filters and built in ventilation. Food and water was available ad libitum.

Immunohistochemistry

Chromogenic immunohistochemistry and immunofluorescence labelling was performed as described previously (Fraser et al. 2017). Briefly, mice were anesthetised and perfused transcardially with phosphate-buffered saline (PBS), followed by 4% paraformaldehyde (PFA), then post-fixed for 48–72 h before long-term storage in PBS at 4 °C. Cerebella were isolated and embedded in 3% Noble agar and sectioned in a sagittal plane at 50 µm intervals using a vibratome. Sections were placed sequentially across the wells of a 6-well plate to ensure appropriate sampling from different medio-lateral regions of the cerebellum. There were between 6 and 8 cerebellar sections per well. Thus, for all analyses we had > 6 sections per animal to image and analyse. Sections were mounted on slides before heat-mediated antigen retrieval was performed in 10 mM sodium citrate solution at 95 °C for 15 min. For chromogenic immunohistochemistry, sections were incubated overnight in primary antibodies at room temperature. A list of antibodies used in this study is given in Table 1. The following day, sections were rinsed in PBS, then incubated in a solution containing a biotinylated secondary antibody (Vector Laboratories) for 1 h at room temperature, followed by processing with a VECTASTAIN ABC kit for 1 h at room temperature (A used at 1/500, B used at 1/500, Vector Laboratories). Sections were rinsed again in PBS, then were processed for colour reaction using a nickel-3,3′-diaminobenzidine (DAB, Sigma) solution (2.5% nickel sulfate and 0.02% DAB in 0.175 M sodium acetate) activated with 0.01% (v/ v) hydrogen peroxide. The colour reaction was stopped by rinsing multiple times with PBS, and sections were then coverslipped with DPX mounting medium (Thermo Fisher Scientific). For IF labelling, sections were incubated at 4 °C overnight with primary antibodies against the target proteins (see Table 1). The following day sections were rinsed in PBS, then incubated with the relevant Alexa Fluor® fluorescent secondary antibodies (Alexa 488 or Alexa 568, 1:250), for 1 h in the dark at room temperature. Sections were rinsed in PBS, then were counterstained with 4′,6-diamidino-2-phenylindole (DAPI), and mounted in fluorescent mounting media (DAKO). For all experiments, at least three animals at each age were analyzed.

Cerebellar imaging

All brightfield images were captured using a Aperio XT Slide scanner and visualized using Aperio ImageScope (Leica Biosystems). For fluorescence images, a Diskovery inverted spinning disk confocal microscope using a 20× objective and a 70-µm pinhole (Nikon TiE; Nikon) was used. We took ten consecutive 1-µm-thick optical sections to generate a 10-µm-thick z-stack. In all cases, the 10-µm z-stack was taken from the middle of the section to minimize potential artefacts arising from the sectioning process such as damage to the tissue. Image acquisition was performed using NIS-elements Advanced Research software (Nikon). For comparative analysis of $Nfix^{-/-}$ and $Nfix^{+/+}$ mice, high magnification images were taken of the same lobe of the cerebellum, using at least five biological replicates at each of the ages assessed. For $Itsn1^{-/-}$ and $Itsn1^{+/+}$ mice, at least three biological replicates were used. For quantification of granule neuron and proliferative markers (PAX6 and Ki67, respectively), three 200 ∝m regions of the EGL were quantified for each section. This ensured more representative count of the EGL thickness. 1 µm-thick optical sections were viewed in Fiji, and the 'cell counter' plugin used to mark and quantify cells expressing respective markers in each fluorescent channel. Cells co-expressing markers (for example, PAX6 and Ki67) were also quantified this way, and DAPI was used to visualize the cell nucleus, to ensure accuracy, especially in areas of high cell density.

Granule cell isolation

GNPs from P7 $Nfix^{+/+}$ and $Nfix^{-/-}$ mice were isolated using the method outlined by Lee et al. (2009) and a papain dissociation kit (Worthington Biochemical Corporation). Briefly, the cerebellum was dissected from three wild-type and three knockout mice and the tissue was dissociated using a 20 units/mL papain solution at 37 °C for 15 min. A single cell suspension was obtained by trituration with a serum-coated

Table 1 Antibodies used in this study

Antibody	Source species	Company	Catalogue number	Dilution used	Purpose
NFIX	Mouse	SIGMA	SAB1401263	1/200;1/1000	IF/IHC
PAX6	Rabbit	Millipore	AB2237	1/400	IF
NEUN	Rabbit	Millipore	MAB377	1/200	IF
GFAP	Rabbit	DAKO	Z0334	1/1000	IF
PHH3	Rabbit	Millipore	06-570	1/400	IF
Ki67	Mouse	BD Pharmigen	550609	1/400	IF

P1000 pipette tip and nuclear membranes were removed using an albumin-ovomucoid inhibitor gradient. GNPs were separated from other cells using a 30–60% percoll gradient. Purified GNP cells were then lysed in Trizol (Ambion) and RNA isolated using an RNeasy miniprep kit (Qiagen). RNA-sequencing was then performed on the samples using the Illumina NextSeq High Output system (Illumina; 150 bp read length, paired-end reads).

RNA-seq analysis

Three RNA-seq replicates each from P7 wild-type GNPs and *Nfix*$^{-/-}$ mice were aligned by TopHat2 (v2.0.9) (Trapnell et al. 2012) to the *Mus musculus*, UCSC, mm10 reference transcriptome and FASTA annotation downloaded from the TopHat index and annotations page (https://ccb.jhu.edu/software/tophat/igenomes.shtml). Cufflinks (v2.1.1) (Trapnell et al. 2012) was used to assemble each replicate's transcripts from the alignment file generated by TopHat. Cuffmerge was used to create a single assembly containing transcripts across all samples and replicates. Cuffdiff was run using the merged set of transcripts and the three replicate TopHat2 bam files from each sample. *Atoh1* differential expression data were obtained from Klisch and colleagues (Klisch et al. 2011), comparing RNA-seq expression of E18.5 wild-type and *Atoh1*$^{-/-}$ cerebellar tissue.

NFIX ChIP-seq

For chromatin immunoprecipitation, litters of P7 pups were pooled for GNP isolation. Isolated GNPs were crosslinked with 1% formaldehyde for 10 min, then were quenched with glycine. Cells were lysed in RIPA buffer supplemented with protease and phosphatase inhibitors (Roche) and sonicated with a Bioruptor (Diagenonde) for six 15-min intervals of 30 s on, 30 s rest. Chromatin immunoprecipitation was performed as described previously (Blythe et al. 2009), using a mouse anti-NFIX antibody (Sigma-Aldrich). We have previously shown the specificity of this antibody using tissue from *Nfix*$^{-/-}$ mice (Chen et al. 2017). Briefly, immunocomplexes were isolated with protein G-agarose beads (Roche), washed once for 5 min with buffers 1 through 4. Crosslinking was reversed by incubation with proteinase K (Roche) at 60 degrees overnight. DNA was isolated by phenol–chloroform extraction then incubated with RNAse A (Roche) for 30 min before final cleanup with PCR columns (Qiagen). Sequencing libraries were constructed using the standard protocol for the NEBNext Ultra II DNA Library Prep Kit for Illumina (New England BioLabs). Pooled libraries were sequenced on an Illumina HiSeq2000 (Illumina; 30 bp single end read).

ChIP-seq analysis

Alignment was performed on both the NFIX ChIP-seq data and ATOH1 ChIP-seq data set (GSE22111) by bowtie2 (Langmead and Salzberg 2012) to mm10. Unaligned reads and reads which aligned to multiple locations were removed leaving only uniquely mapped reads. MACS2 (Feng et al. 2012) was used to call narrow peaks with default parameters for both datasets. Both experiments contained two biological replicates and if both biological replicates shared a peak, it was recorded using the maximum boundaries of the supporting peaks to generate a merged set of peaks for each experiment. Uniform 500 bp peaks from the NFIX ChIP-seq data were created using a ± 250 bp window around peak centres. This uniform set of peaks was input to MEME Suite to perform de novo motif discovery using MEME-ChIP version 5.0.1 (Bailey et al. 2009; Machanick and Bailey 2011).

Annotation of ChIP-seq peaks

A set of target genes were identified for both NFIX and ATOH1 by the following method. A promoter region was defined as ± 2000 base pairs around a transcription start site. ChIP-seq binding sites located in a promoter region were annotated as proximal, while sites outside the promoter region but overlapping gene boundaries (transcription start to stop) were labelled as genic. All remaining binding sites were labelled as distal. A binding site annotated as proximal was assigned the nearest gene as a target while genic-binding sites were assigned the overlapping gene as a target. Distal-binding sites are difficult to assign target genes to, as they are not necessarily regulating the nearest gene (by genomic distance). CisMapper was used to annotate distal binding sites and provide a secondary annotation to proximal and genic sites, with resulting links filtered to a threshold of 0.05 (O'Connor et al. 2017).

After identifying a gene target for each NFIX binding site; the associated p value from both the *Nfix* and *Atoh1* RNA-seq differential expression analyses was recorded. Genes targeted by both *Nfix* and *Atoh1* with a significant ($p < 0.05$) change in expression in both experiments were extracted. Genes showing coordinated positive or negative log fold change values across both experiments were selected to generate a putative set of genes under the control of *Nfix* and *Atoh1*. Functional annotation was performed using DAVID (6.8) on target genes identified for *Nfix* (Huang da et al. 2009a, b).

DNase I hypersensitivity analysis

DNase I hypersensitivity (DHS) called peaks from whole cerebellum at P7 across three replicates were retrieved from Frank et al. 2015 (GEO: GSE60731). UCSC liftover was

used to convert the mm9 files to mm10. If at least two replicates shared a peak, it was recorded using the maximum boundaries of the supporting peaks to generate a merged DHS peak file. Transcription factors are known to bind preferentially in regions of accessible chromatin (Guertin and Lis 2013; Hughes 2011) and DHS was therefore used to extract NFIX ChIP-seq peaks occurring in accessible regions.

Neurosphere assays

GNPs were isolated from P7 wild-type and *Nfix*$^{-/-}$ mice and were seeded into a T25 flask in neurobasal stem cell medium containing 20 ng/mL of epidermal growth factor (EGF), 10 ng/mL of basic fibroblast growth factor (bFGF) and 3.5 µg/mL of heparin. After 7 days, neurospheres were dissociated using trypsin to form a single cell suspension. Cells were counted and seeded at a density of 2.5×10^5 cells per T25 flask. Cells were passaged until passage three. Neurospheres were counted and sphere diameter was measured at each passage.

Medulloblastoma cell lines

The medulloblastoma cell lines DAOY, D283, and UW228 were maintained in RPMI medium containing 10% foetal bovine serum. The MB4 primary cell line was maintained in StemPro NSC SFM media (Thermo Fisher). 2.5×10^5 cells were seeded into a 6-well plate and cells were lysed in Trizol (Ambion) after 48 h. RNA was extracted using the RNAeasy miniprep kit (Qiagen). cDNA was prepared from RNA isolated from the medulloblastoma cell lines using a Superscript III Reverse Transcription kit (Invitrogen). cDNA was transcribed from human cerebellum RNA (Clontech) and used as a control for comparison of gene expression levels. qPCR was performed with the Quantifast SYBR kit (Qiagen). Gene expression was calculated using $2^{-\Delta\Delta Ct}$ method relative to the housekeeping gene *glyceraldehyde 3-phosphate dehydrogenase* (*GAPDH*).

qPCR analysis of target genes

RNA isolated from GNPs of wild-type and *Nfix*$^{-/-}$ mice at P7 was used to prepare cDNA as described previously (Piper et al. 2014). qPCR was performed with Quantifast SYBR Green (Qiagen) to detect gene expression levels of the genes identified in the RNA-seq analysis. The primers for these genes are listed in Table 2. Gene expression was calculated using $2^{-\Delta\Delta Ct}$ method relative to the housekeeping gene *glyceraldehyde 3-phosphate dehydrogenase* (*Gapdh*). All the samples were tested in triplicate within each experiment, and each experiment was repeated three times.

Results

Delayed EGL differentiation in the cerebellum of postnatal Nfix$^{-/-}$ mice

In our preliminary description of the cerebellar phenotype of *Nfix*$^{-/-}$ mice, we demonstrated that these mice have reduced numbers of PAX6-positive GNPs in the EGL at P5 in comparison to wild-type controls (Piper et al. 2011). Within the embryonic forebrain of these mutant mice, radial glial progenitor cells exhibit delayed differentiation (Dixon et al. 2013; Harris et al. 2016). We hypothesized that GNPs within the EGL would exhibit a similar delay in differentiation within *Nfix*$^{-/-}$ mice. To test this hypothesis, we used PAX6-immunocytochemistry to visualize GNPs within the EGL of P5, P10 and P15 wild-type and *Nfix*$^{-/-}$ mice. At P5, there were fewer GNPs in the EGL of mutant mice in comparison to controls, whereas at P10, the number of these cells in

Table 2 qPCR primers used in this study

Gene	Forward	Rev
Itsn1	TCAGTTTCCCACACCTTTCG	TCAGGCTAAGGAACTGCTGG
Kit	CACATACACGTGCAGCAACA	GAAGGCCAACCAGGAAAAGT
Serpine2	ACGGCAAGACAAAGAAGCAG	AGCCTTGTTGATCTTCTTCAGC
Dab1	AACCAGCGCCAAGAAAGAC	ATCAGCTTGGCTTTGTACCG
Hes1	TCTGAGCACAGAAAGTCATCA	AGCTATCTTTCTTAAGTGCATC
Dll1	TTCTCTGGCTTCAACTGTGAG	CATTGTCCTCGCAGTACCTC
Notch3	AGTGCCGATCTGGTACAACTT	CACTACGGGGTTCTCACACA
Neurod1	ATGACCAAATCATACAGCGAGAG	TCTGCCTCGTGTTCCTCGT
Rbfox3	GGCAAATGTTCGGGCAATTCG	TCAATTTTCCGTCCCTCTACGAT
Gapdh	GCACAGTCAAGGCCGAGAAT	GCCTTCTCCATGGTGGTGAA
NFIX	AGGACTGTTTTGTGACTTCCG	GGTTGATGTTGTAGTAGCTGGG
GAPDH	CCCTTCATTGACCTCAACTACAT	TCCTGGAAGATGGTGATGG
ITSN1	GGGCCATAACTGTAGAGGAAAGA	ACAGGTTGAGGTAACCCAGAT

both genotypes was comparable (Fig. 1a–d). Interestingly, at P15 there were more PAX6-positive cells in the EGL of the mutant in comparison to the control (Fig. 1e, f), indicative of delayed GNP differentiation.

To quantify this phenotype, we performed co-immunofluorescence labelling against PAX6 and the proliferation marker, Ki67, followed by confocal microscopy. We performed cell counts within the EGL on confocal optical sections of the emerging cerebellum. At P5, there were significantly more cells expressing PAX6 and Ki67 in the wild-type EGL compared to the mutant (Fig. 2a–j). At P10, however, the numbers of PAX6-positive cells and proliferating cells within the EGL was not significantly different between genotypes (Fig. 2k–t). In contrast, there were significantly more GNPs within the EGL of P15 *Nfix*$^{-/-}$ mice compared to the control, as the majority of these cells had differentiated in wild-type mice by this age (Fig. 2u–dd). A similar trajectory of GNP differentiation was observed when we used a second marker for proliferation, the mitotic marker phosphohistone H3 (PHH3; Fig. 3).

Nfix $^{-/-}$ GNPs exhibit increased proliferation in vitro

These findings led us to posit that NFIX mediates GNP differentiation, and that the absence of this gene could lead to elevated GNP proliferation, as has been previously reported in the embryonic hippocampus of *Nfix*$^{-/-}$ mice (Harris et al. 2016). To test this hypothesis, we isolated GNPs from the EGL of P7 wild-type and *Nfix*$^{-/-}$ mice using papain dissociation and a percoll gradient (Lee et al. 2009; Fraser et al. 2017). We performed qPCR on cDNA generated from this tissue, and revealed that the expression of the stem cell markers *Hes1* and *Notch 3* was significantly elevated in GNPs isolated from P7 *Nfix*$^{-/-}$ mice in comparison to controls (*Hes1*: control 0.0051 ± 0.0001, *Nfix*$^{-/-}$ 0.0079 ± 0.0003; *Notch 3*: control 0.0023 ± 0.0001, *Nfix*$^{-/-}$ 0.0038 ± 0.0002; $p < 0.01$, *t* test). Moreover, the analysis of two markers for neuronal differentiation, *Neurod1* and *NeuN* (*Rbfox3*) revealed significantly reduced expression of these factors in GNPs isolated from P7 *Nfix*$^{-/-}$ mice in comparison to controls (*Neurod1*: control 0.53 ± 0.01, *Nfix*$^{-/-}$ 0.37 ± 0.002; *Rbfox3*: control 0.13 ± 0.003, *Nfix*$^{-/-}$ 0.005 ± 0.004; $p < 0.01$, *t* test). Next, we used the percoll gradient protocol to again isolate GNPs from the EGL of P7 wild-type and *Nfix*$^{-/-}$ mice and cultured these cells in a neurosphere assay. We cultured cells for three passages, and quantified both the number of spheres, as well as sphere diameter. At each passage, there were significantly more spheres in cultures derived from *Nfix*$^{-/-}$ EGL progenitors in comparison to controls (Fig. 4a–c). Furthermore, whereas the majority of wild-type spheres were less than 50 µm in diameter, in the mutant, the majority of spheres were over 70 µm in diameter (Fig. 4d). Interestingly, the expression of GFAP by developing Bergmann glia was also delayed in the absence of *Nfix* [Supp. Figure 1; (Piper et al. 2011)], suggesting that a delay in glial differentiation could also potentially underlie the accumulation of PAX6-positive cells within the EGL of *Nfix*$^{-/-}$ mice. However, our neurosphere data clearly indicate elevated levels of proliferation in GNPs isolated from *Nfix*$^{-/-}$ cerebella, indicating that NFIX plays a central role in mediating the differentiation of cerebellar GNPs.

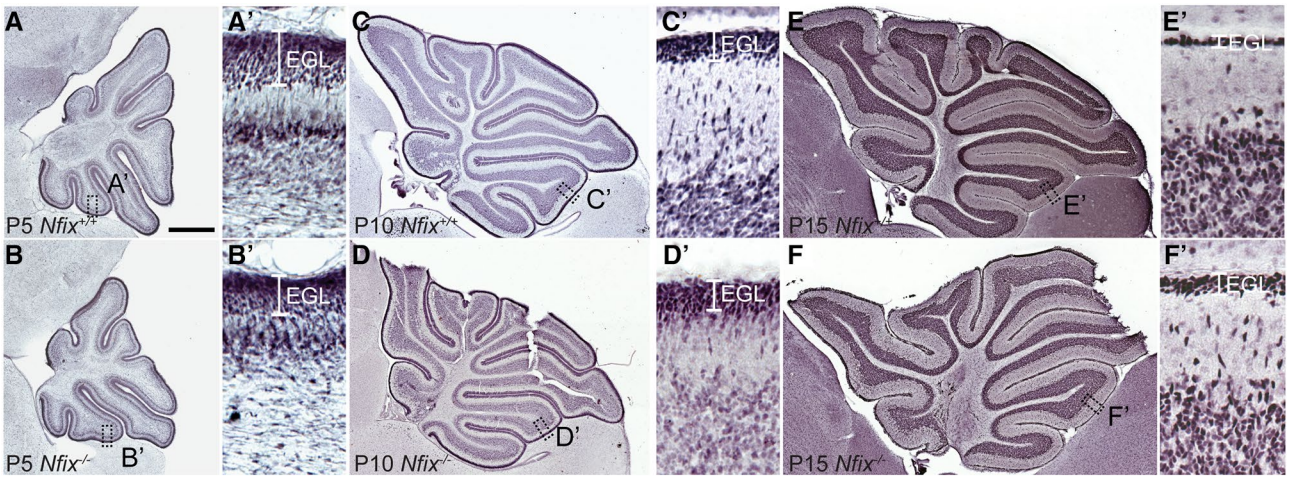

Fig. 1 Delayed differentiation of GNPs in the cerebellum of *Nfix*-deficient mice. Mid-sagittal sections of P5 (**a**–**b'**), P10 (**c**–**d'**) and P15 (**e**–**f'**) wild-type (**a, c, e**) and *Nfix*$^{-/-}$ (**b, d, f**) mice stained with antibodies against PAX6. The boxed regions in A-F are shown at higher magnification in **a'**–**f'** respectively. The morphology of the cerebellum appeared grossly normal in mice lacking *Nfix*. However, higher magnification views of the external granule layer (EGL) revealed that this germinal zone was thinner at P5 in mutant mice. At P10 the EGL of the mutant was comparable to the control. At P15, whereas the EGL was almost completely depleted in the wild-type, there were still numerous PAX6-positive cells in this cellular layer of *Nfix*$^{-/-}$ mice. Scale bar (in **a**) **a**–**f** = 250 µm, **a'**–**f'** = 25 µm

Mutations in another NFI family member, *Nfia*, have previously been implicated in medulloblastoma, a paediatric cancer of the cerebellum (Genovesi et al. 2013). Using a Sleeping Beauty transposon screen, Genovesi and colleagues revealed that mutations to *Nfia* led to reduced latency of medulloblastoma formation in a *Ptch1*$^{+/-}$ background. Transposon insertions were also identified within the *Nfix* locus in this screen (Genovesi et al. 2013), but the role of *NFIX* in medulloblastoma is poorly defined. In light of our data in the developing cerebellum, we analyzed *NFIX* expression in three medulloblastoma cell lines (DAOY, UW228 and D238), and a primary medulloblastoma cell line (MB4). *NFIX* mRNA was significantly reduced in comparison to control mRNA isolated from the adult cerebellum (Fig. 4e). A similar reduction in expression was also obtained when we analyzed the expression of the other NFI family members, *NFIA, NFIB* and *NFIC* (data not shown). Collectively, these data are consistent with the in vivo cerebellar phenotype of *Nfix*$^{-/-}$ mice, and suggest that NFIX acts to drive the differentiation of cerebellar GNPs.

Transcriptomic profiling reveals a broad suite of potential targets of NFIX within GNPs

To define transcriptional targets for NFIX during GNP differentiation, we undertook a range of bioinformatic approaches using both published, and newly generated, transcriptomic data, aimed at defining a small list of high-confidence targets that we could experimentally validate. To determine the transcriptomic landscape in GNPs lacking *Nfix*, we first isolated GNPs from both wild-type and *Nfix*$^{-/-}$ cerebella at P7, and performed transcriptomic profiling (RNA-seq) on the RNA isolated from these cells. Analysis revealed 1402 genes as being significantly misregulated in *Nfix*$^{-/-}$ GNPs in comparison to controls (Fig. 5a, Supp. Table1). Gene Ontology and Pathway analyses of these genes using DAVID (Huang da et al. 2009a, b) identified a diverse range of processes potentially controlled by NFIX within GNPs, including cell adhesion, extracellular matrix organisation and axon guidance (Fig. 5b).

To determine direct targets of NFIX in GNP differentiation, we next performed ChIP-seq on DNA derived from isolated P7 GNP preparations using an anti-NFIX antibody whose specificity has been previously demonstrated (Chen et al. 2017; Vidovic et al. 2018). This experiment identified 6910 specific NFIX binding peaks (Fig. 5c, Supp. Table 2). Interestingly, a recent publication used DNase 1 hypersensitivity analysis on whole cerebellar tissue to investigate chromatin accessibility within these cells at different stages in development (Frank et al. 2015). We posited that NFIX ChIP-seq peaks identified within regions of open chromatin would be more likely to regulate gene transcription directly. As such, we filtered our NFIX ChIP-seq data using the DNase 1 hypersensitivity data from P7 (Frank et al. 2015), an analysis that revealed that 5843 of the NFIX ChIP-seq peaks were found in regions of accessible chromatin at this age (Fig. 5c, Supp. Table 2). Finally, the intersection of the differentially expressed genes identified via RNA-seq (Fig. 5a) with those genes identified as having an NFIX ChIP-seq peak in an accessible region of chromatin (Fig. 5c) identified 578 genes as being potential targets for direct NFIX-mediated regulation within P7 GNPs (Fig. 5d, Supp. Table 3). This analysis revealed a number of genes previously implicated in cerebellar development, such as *Otx2* and *Dab1*, as well as a range of genes whose role in cerebellar development has not been previously studied (e.g. *Heg1, Tiam2*). Interestingly, *Nfix* was also identified via this filtering analysis, suggesting that NFIX autoregulates its own expression within the context of GNP development.

To search for further ways in which we could refine our list of potential NFIX target genes, we performed motif discovery and enrichment analyses (Bailey et al. 2009; Machanick and Bailey 2011) on the NFIX binding peaks isolated in our ChIP-seq experiment. As expected, the conserved motif bound by NFI transcription factors (Heng et al. 2012) was identified as being enriched in our ChIP-seq peaks. Interestingly, we also observed enrichment of the ATOH1 binding motif within NFIX ChIP-seq peaks (Fig. 6a). ATOH1 is strongly and specifically expressed by GNPs, and has previously been shown to regulate the proliferation of these cells, as well as concomitantly priming them for differentiation (Klisch et al. 2011). This finding indicates that NFIX and ATOH1 could potentially regulate a common suite of genes developmentally. Given this, we postulated that we could use the analysis of ATOH1 target genes to further refine our list of potential NFIX targets. To do this, we used a recent analysis of the ATOH1 targetome in cerebellar tissue (Klisch et al. 2011). This study mapped differential gene expression in E18.5 cerebellar tissue isolated from *Atoh1*-deficient mice, as well as identifying potential direct targets of ATOH1 by performing ChIP-seq on P5 cerebellar tissue (Klisch et al. 2011). Analysis of these two sequencing datasets identified 1551 genes as potential ATOH1 targets (i.e. the target gene contained at least one ATOH1 ChIP-seq peak, and was significantly differentially expressed in E18.5 *Atoh1*$^{-/-}$ cerebellar tissue; Fig. 6b) (Klisch et al. 2011). The comparison of these potential ATOH1 target genes with those 578 NFIX target genes identified in our RNA-seq and ChIP-seq analyses (Fig. 5d; Supp. Table 3) revealed 177 genes as potential targets of both ATOH1 and NFIX in cerebellar development. Critically, 90 of these genes were coordinately misregulated in both *Nfix*$^{-/-}$ GNPs and *Atoh1*$^{-/-}$ cerebellar tissue (Fig. 6b, c). This list of putative NFIX targets included *Nfix* itself, as well as other factors previously implicated in cerebellar development, including *Otx2, Robo1* and *Dab1* (Vernay et al. 2005; Gallagher et al. 1998; Tamada et al. 2008).

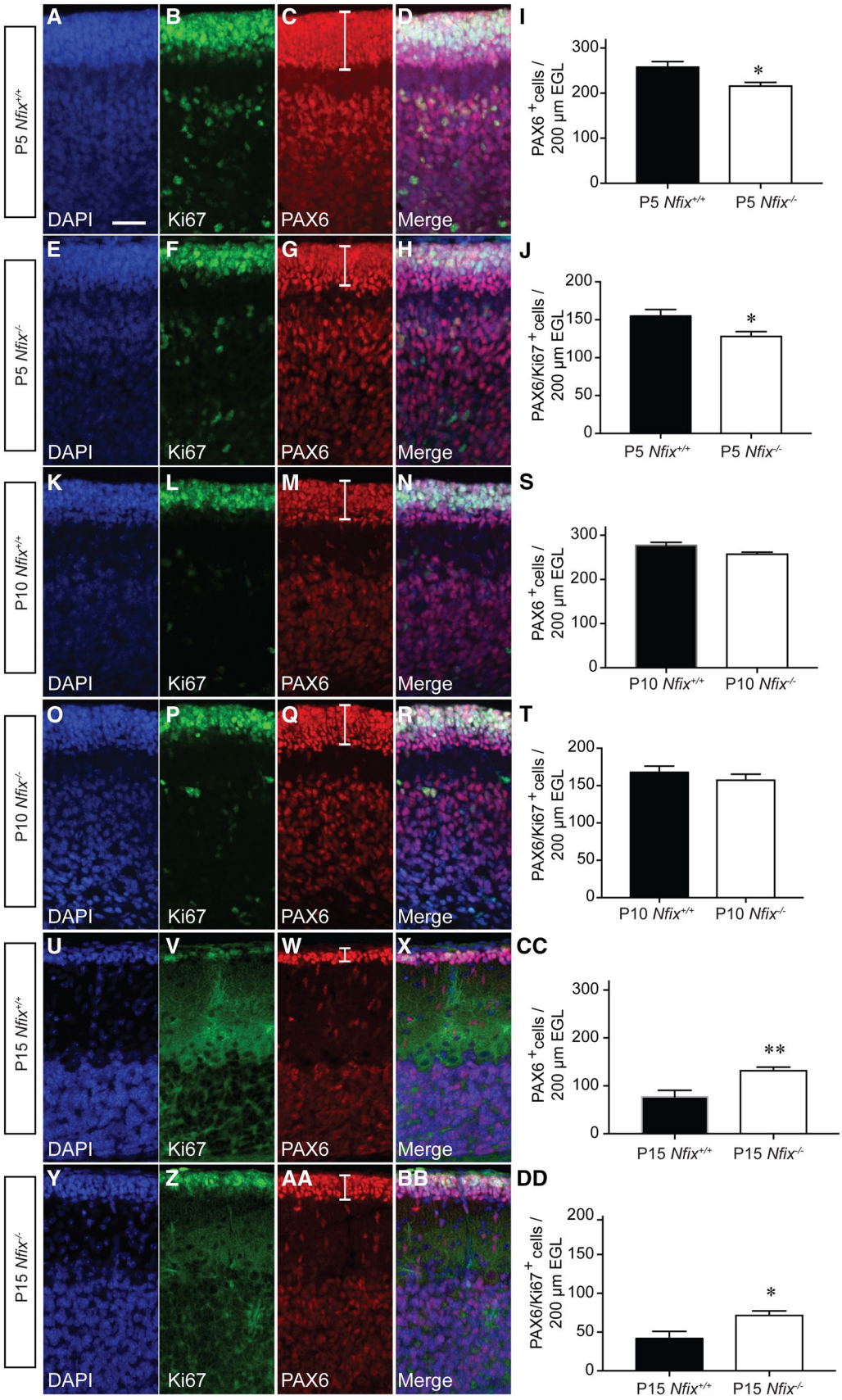
P5 Nfix+/+
P5 Nfix-/-
P10 Nfix+/+
P10 Nfix-/-
P15 Nfix+/+
P15 Nfix-/-
DAPI
Ki67
PAX6
Merge
I
J
S
T
CC
DD
PAX6+ cells / 200 µm EGL
PAX6/Ki67+ cells / 200 µm EGL
P5 Nfix+/+
P5 Nfix-/-
P10 Nfix+/+
P10 Nfix-/-
P15 Nfix+/+
P15 Nfix-/-

◂**Fig. 2** Retention of GNPs in late postnatal *Nfix*$^{-/-}$ mice. Expression of the nuclear marker DAPI (blue), the proliferative marker Ki67 (green), and PAX6 (red), a marker of GNPs and their progeny, in P5 (**a**–**h**), P10 (**k**–**r**) and P15 (**u**–**bb**) mice. The EGL in delineated by brackets in panels **c, g, m, q, w** and **aa**. At P5 there were significantly more PAX6-positive cells (**i**) and PAX6/Ki67 double-positive cells (**j**) in the wild-type EGL in comparison to the mutant. At P10, there were no significant differences in either PAX6- (**s**) or PAX6/Ki67-expressing (**t**) cells between groups. At P15, however, there were significantly more PAX6-positive cells (**cc**) and PAX6/Ki67 double-positive cells (**dd**) in the EGL of *Nfix*$^{-/-}$ mice in comparison to the control. $^{*}p < 0.05$, *t* test. Scale bar (in **a**) = 25 µm

Interestingly, this analysis also revealed a range of genes that have not previously been implicated in cerebellar development, including *Coro2b*, and *intersectin 1* (*Itsn1*; Fig. 6d).

Intersectin 1 is a target for transcriptional activation by NFIX during GNP differentiation

Of those novel factors identified in our transcriptomic screens, *Itsn1* was of particular interest to us. This gene encodes a multi-domain scaffold protein that has been implicated in regulating numerous cellular signalling pathways (Herrero-Garcia and O'Bryan 2017). With relation to neuronal development, *Itsn1* has been implicated in connectivity at the cortical midline of the dorsal telencephalon, with deficiencies to this gene correlated with aberrant higher order cognition (Sengar et al. 2013). Mechanistically, *Itsn1* has recently been implicated in neuronal migration within the hippocampus as part of the reelin signalling pathway, via its interaction with the reelin receptor VLDLR, and with Dab1, a signalling molecule downstream of VLDLR (Jakob et al. 2017). Given the importance of reelin signalling for cerebellar development (Vaswani and Blaess 2016), and the identification of *Dab1* in our transcriptomic screen, we focussed on *Itsn1* as a target for NFIX in GNP differentiation. We first validated our RNA-seq dataset by performing qPCR on GNPs isolated from independent P7 *Nfix*$^{-/-}$ and control cerebella (Fig. 7a). In line with our sequencing results, *Itsn1* mRNA was significantly reduced in *Nfix*$^{-/-}$ samples in comparison to controls, whereas the mRNA levels of *Kit, serpine 2* and *Dab1* were significantly increased in the mutant. These data suggest that NFIX acts to promote the expression of *Itsn1* during GNP differentiation. If this was the case, we would hypothesize that mice lacking *Itsn1* would potentially phenocopy those lacking *Nfix* with regards to cerebellar development. To test this hypothesis, we analysed the cerebellum of *Itsn1*$^{-/-}$ mice at P15. Hematoxylin staining revealed that foliation of the cerebellum was grossly normal in these mice in comparison to controls (Fig. 7b, c). However, closer analysis of the EGL of mutant mice revealed that the EGL of *Itsn1*$^{-/-}$ mice at P15 was markedly thicker when compared to control mice (7B', C'). Indeed, immunofluorescence labelling with PAX6, followed by confocal microscopy, revealed significantly more GNPs within the EGL of *Itsn1*$^{-/-}$ mice at this age than controls (Fig. 7d–j). Similarly, there were significantly more Ki67-expressing cells in the EGL of mutant mice at this age in comparison to wild-type controls (Fig. 7k). The expression of GFAP by Bergmann glia was comparable between wild-type and *Itsn1*$^{-/-}$ mice at this age (Supp. Fig. 2), although it is possible that GFAP expression was reduced at earlier time points akin to what we observed with the *Nfix* mutant, and that this may also have contributed to the enlarged EGL at P15 in the absence of *Itsn1*. Finally, like *NFIX*, the expression of *ITSN1* was also significantly reduced in medulloblastoma cell lines (Fig. 7l). Collectively, these data, in association with our RNA-seq and ChIP-seq analyses, suggest that NFIX-mediated regulation of *Itsn1* plays an important role in GNP differentiation during cerebellar development.

Discussion

Studies into the role of the NFI family in cerebellar development have highlighted a key role for these transcription factors in mediating neuronal migration and synaptic maturation (Kilpatrick et al. 2012). Here, we extend these findings, revealing that NFIX regulates GNP biology within the postnatal cerebellum. Indeed, the delayed differentiation of GNPs in vivo in *Nfix*-deficient mice, coupled with the elevated proliferation of *Nfix*$^{-/-}$ GNPs in vitro, are supportive of a role for NFIX in promoting timely GNP differentiation within the postnatal cerebellum. This is in accordance with studies into the role of the NFI family during nervous system development (Fane et al. 2017; Harris et al. 2015), with impairments in neural stem cell differentiation observed in the absence of NFIs from diverse regions of the brain, including the neocortex (Piper et al. 2009), hippocampus (Heng et al. 2014; Piper et al. 2014) and spinal cord (Matuzelski et al. 2017). Collectively, these data implicate the NFI family, including NFIX, as key drivers of neural development via the promotion of neural stem cell differentiation.

How do NFIs drive this process at a mechanistic level? A number of studies have investigated the roles these factors play during nervous system development. Early studies using *Nfi*-deficient mice revealed severe delays in astrocyte differentiation, suggesting a central role for this family in gliogenesis within the cerebral cortex and spinal cord (Deneen et al. 2006; Shu et al. 2003). More recently, transcriptional profiling experiments such as microarrays, coupled with molecular analyses and bioinformatics, have identified a range of target genes in the developing and adult nervous system that act to either repress stem cell identity or to promote cellular differentiation (Harris et al. 2018, 2016). These include *Apcdd1, Mmd2* and *Zcchc24* (spinal cord) (Kang et al. 2012), *Insc, Sox9* and *Ezh2*

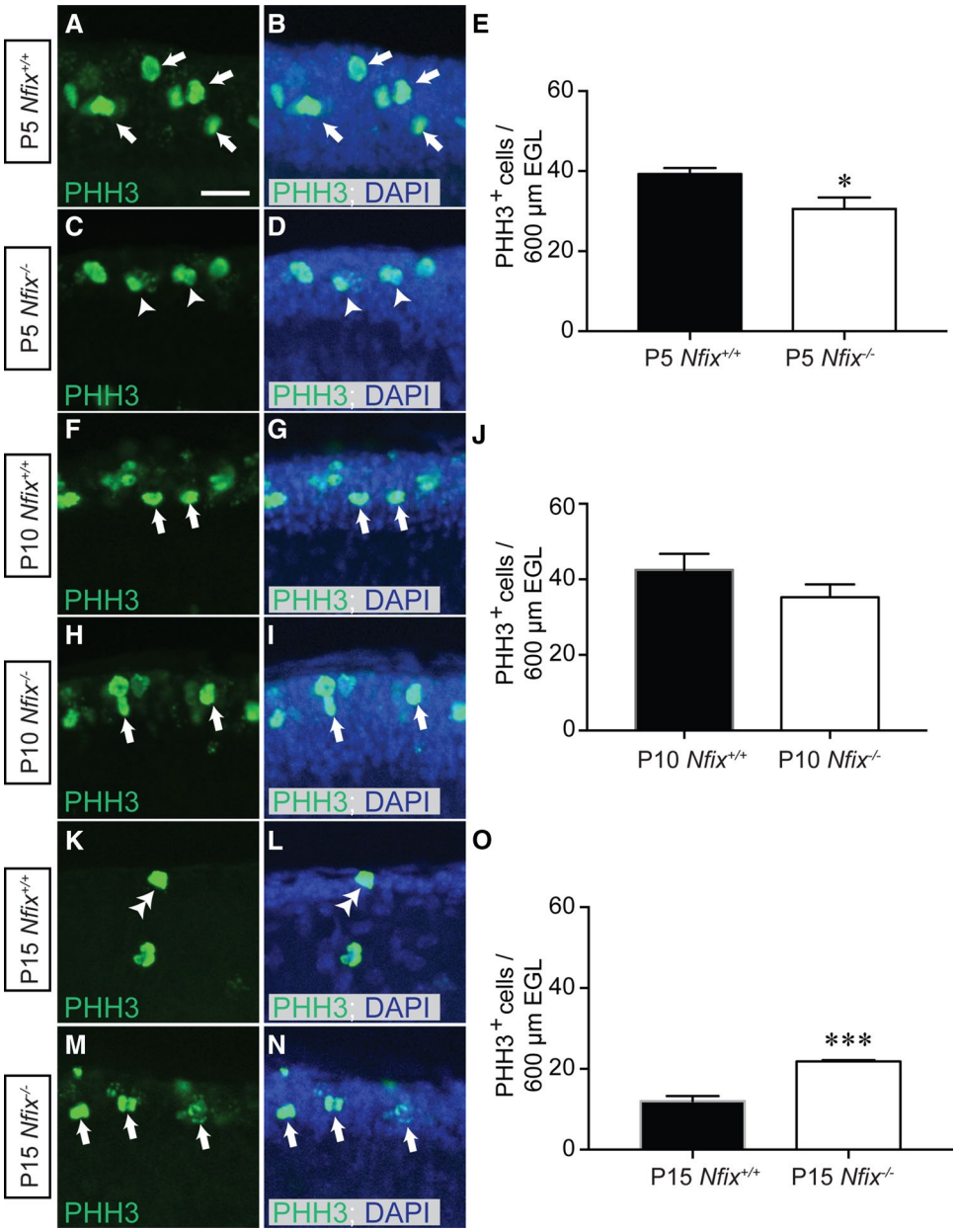

Fig. 3 Delayed proliferation profile of GNPs in the absence of *Nfix*. Transverse sections of P5 (**a**–**d**), P10 (**f**–**i**) and P15 (**k**–**n**) wild-type and mutant cerebella labelled with DAPI (blue) and antibodies against the proliferative marker phosphohistone H3 (PHH3). At P5, there were significantly more proliferating cells in the EGL of the wild-type (arrows in **a, b**) in comparison the control (arrowheads in **c, d**; quantified in **e**). At P10, however, the rate of proliferation within the EGL was comparable between sample wild-types and mutants (arrows in **f**–**i**; quantified in **j**). At P15, the situation was reversed, with there being significantly fewer proliferating cells within the EGL of wild-type mice (double arrowheads in **k, l**) in comparison to mutant mice (arrows in **m, n**; quantified in **o**). *$p < 0.05$, ***$p < 0.001$ *t* test. Scale bar (in **a**) = 25 µm

and (hippocampus) (Harris et al. 2016; Heng et al. 2014; Piper et al. 2014), as well as *Bbx* and *Hes1* (cerebral cortex) (Dixon et al. 2013; Piper et al. 2010). The advent of genome-wide profiling using techniques such as RNA-seq and ChIP-seq now means that the direct targets of transcription factors like NFIX can be investigated globally in a more rigorous manner. To the best of our knowledge, this is the first study that has investigated downstream targets of a specific NFI family member within the nervous system using these techniques co-operatively. Moreover, when coupled with available data relating to chromatin accessibility (Frank et al. 2015) and the ATOH1 targetome (Klisch et al. 2011), this study provides a significant conceptual advance in our understanding of the transcriptional landscape regulated by NFIX within the postnatal cerebellum.

One of the novel targets identified as a potential regulator of GNP biology downstream of NFIX using these techniques was the scaffold protein intersectin 1. The gene coding for this factor contained NFIX ChIP-seq peaks near its 3′ UTR, and was significantly downregulated in the absence of *Nfix*. Moreover, mice lacking *Itsn1* phenocopied $Nfix^{-/-}$ mice with regards to delayed differentiation of GNPs within the postnatal EGL. These data suggest that ITSN1 contributes to the differentiation of GNPs. At this stage, it is unclear precisely how ITSN1 regulates the differentiation of GNPs. However, given the nature of this protein as a scaffold capable of binding and influencing many signalling pathways

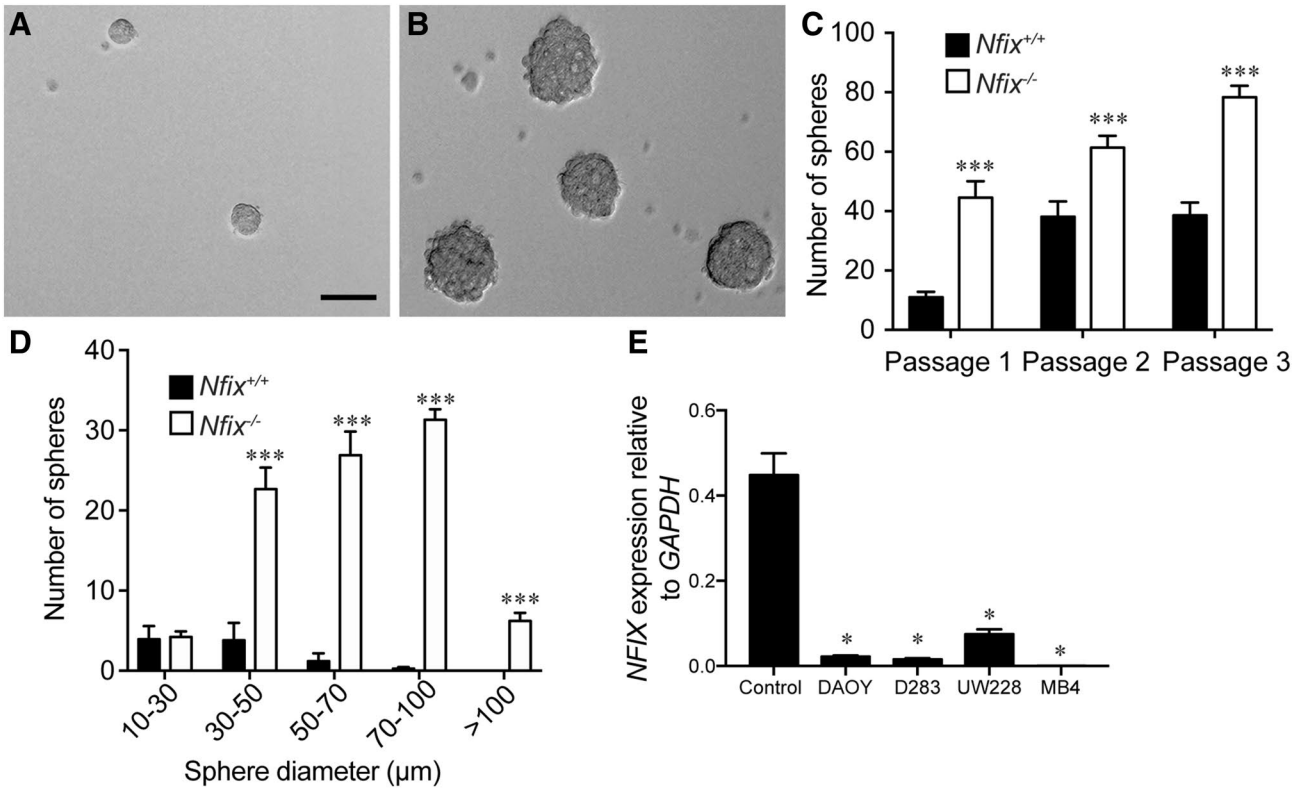

Fig. 4 *Nfix*$^{-/-}$ GNPs exhibit elevated proliferation in vitro. GNPs were isolated from P7 wild-type and *Nfix*$^{-/-}$ cerebella and were cultured in a neurosphere assay for multiple passages. At passage 3, wild-type spheres (**a**) were smaller and fewer in number than those derived from *Nfix*$^{-/-}$ GNPs (**b**). Indeed, there were significantly more spheres derived from *Nfix*$^{-/-}$ GNPs at each passage in comparison to the control (**c**). Moreover, at passage 3, spheres derived from *Nfix*$^{-/-}$ GNPs were on average larger than controls (**d**). **e** qPCR revealed that different medulloblastoma cell lines had significantly lower *NFIX* expression in comparison to normal cerebellar tissue. *$p<0.05$, ***$p<0.001$ ANOVA. Scale bar (in **a**) = 30 μm

(Herrero-Garcia and O'Bryan 2017), there are many potential means by which ITSN1 could mediate GNP differentiation. For example, ITSN1 has been shown to regulate Ras family GTPases, including Ras, with ITSN1 postulated to promote Ras activation (Adams et al. 2000). As RAS signalling has previously been shown to be required for the proliferation of GNPs postnatally (Sanchez-Ortiz et al. 2014), abnormal activation of this factor, and the downstream ERK-MAPK pathway, may potentially contribute to the phenotype evident in these mice. ITSN1 has also been shown to mediate caveolin-mediated endocytosis (Gubar et al. 2013). This may be particularly pertinent for GNP biology, as the continued proliferation of these cells is controlled, at least in part, by sonic hedgehog (Shh) released by Purkinje cells (Roussel and Hatten 2011). Endocytosis of the Shh receptor, Ptch1, to the lysosome plays a key role in continued GNP proliferation (Yue et al. 2014). It is feasible that ITSN1 may contribute to this process. Looking forwards, proteomic studies performed on postnatal GNPs will provide a framework in which to understand the molecular partners of ITSN1, and so the processes this scaffold protein may regulate in vivo.

Our findings also suggest a potential role for *NFIX* in medulloblastoma, a malignant childhood cancer of the cerebellum. Another NFI family member, NFIA, was recently linked to the formation of medulloblastoma using a Sleeping Beauty transposon screen to identify genetic modifiers of tumour formation in *Ptch1* heterozygous mice (Genovesi et al. 2013). This study also identified *Nfix* as being significantly enriched as a tumour suppressor. In humans, recent gene expression analyses of patient medulloblastoma samples revealed that *NFIX* expression is significantly lower in type 3α and type 3γ medulloblastomas, subtypes with poor prognosis and increased frequency of metastasis (Cavalli et al. 2017). Although both of these studies identified NFIX, Shh and type 3 medulloblastoma subgroups are characterised by different oncogenic drivers. However, preliminary data suggest that Hedgehog-dependent tumours, including medulloblastomas and basal cell carcinomas, are capable of switching oncogenic pathways, and hence becoming more metastatic (Ransohoff et al. 2015; Zhao et al. 2015). It remains to be tested whether NFI family members play a role in this transition, or appear as tumour suppressors solely

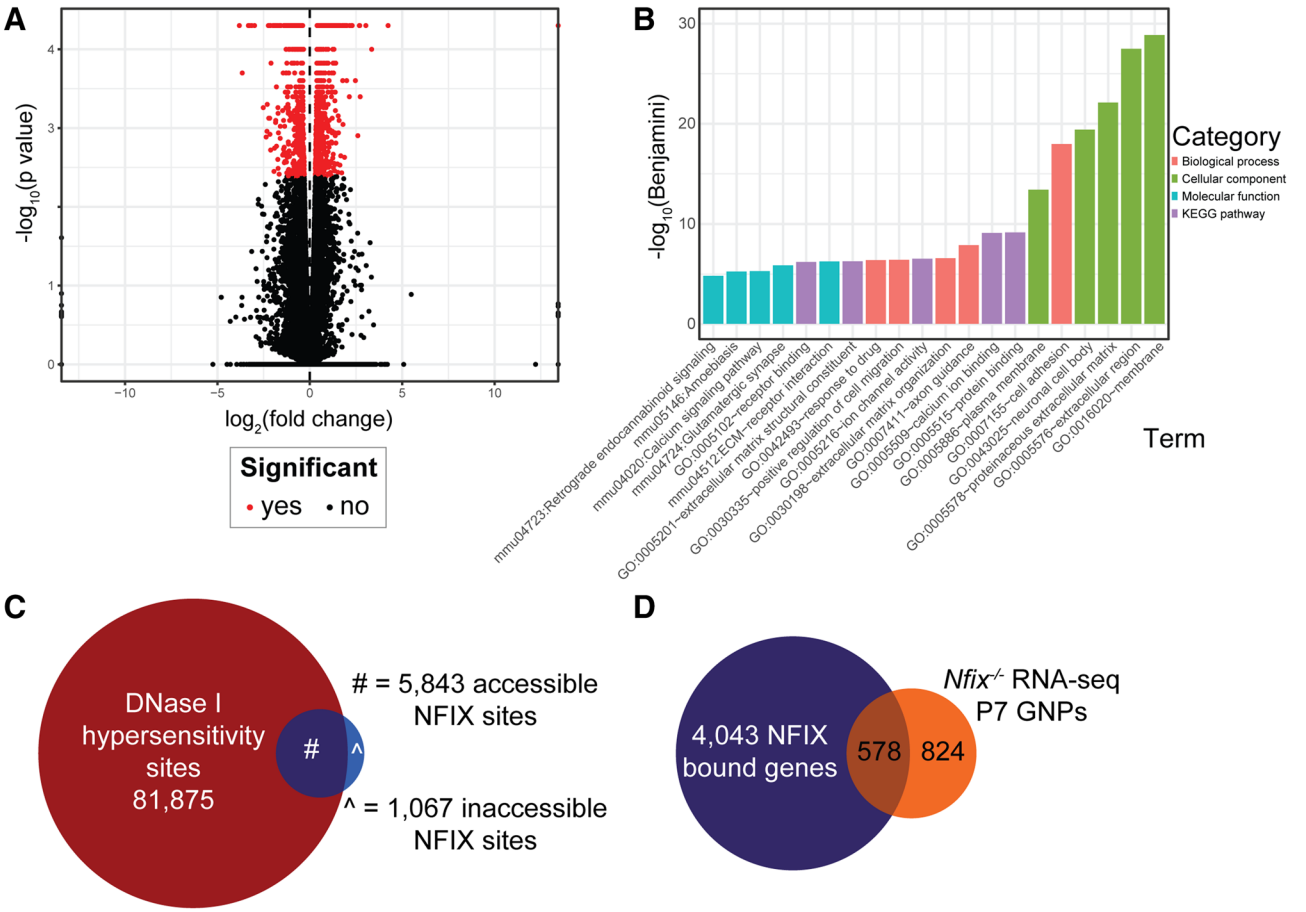

Fig. 5 Transcriptomic profiling of *Nfix*$^{-/-}$ GNPs. **a** Volcano plot representing the transcriptional profile of P7 *Nfix*$^{-/-}$ GNPs in comparison to controls. Red dots represent the 1402 significantly misregulated genes in P7 *Nfix*$^{-/-}$ GNPs as identified by RNA-sEq. **b** Gene Ontology (DAVID 6.8) analysis, showing those biological processes, cellular components and molecular functions misregulated in P7 *Nfix*$^{-/-}$ GNPs, as well as KEGG pathways identified as being abnormal in these cells. **c** To narrow the list of potential NFIX target genes, we performed ChIP-seq on wild-type P7 GNPs with an anti-NFIX antibody. This revealed 6910 NFIX binding peaks. We compared this with a published DNase I hypersensitivity analysis of P7 cerebellar tissue (Frank et al. 2015). Of the 6910 ChIP peaks, 5843 were in regions of accessible chromatin. We then compared the 4621 genes associated with these 5843 NFIX peaks with our RNA-seq data (**a**). This analysis identified 578 potential NFIX target genes (**d**)

due to their pro-differentiation roles. Furthermore, haploinsufficiency to *NFIX* in human patients culminates in Malan Syndrome, a disorder characterised by overgrowth of many organ systems, including the brain (Klaassens et al. 2015; Malan et al. 2010). This implies a pro-differentiation role for NFIX during development, and is consistent with our work on NFIX in the cerebellum.

A key advance we have made in this work is to use RNA-seq, ChIP-seq (this study) and chromatin accessibility (Frank et al. 2015) to define the potential targets of NFIX during development. This approach enabled us to identify 5843 high-confidence NFIX ChIP-seq peaks. Through the combination of our RNA-seq analysis, these high-confidence peaks were subsequently linked to 578 target genes. Motif discovery further led us to identify ATOH1 as a factor that may bind to similar genes as NFIX during GNP development. Published data pertaining to the loss of *Atoh1* expression (Klisch et al. 2011) revealed that *Nfix* is downregulated in *Atoh1*$^{-/-}$ cerebellar tissue, suggesting that ATOH1 potentially regulates *Nfix* expression. Indeed, a number of genes were commonly misregulated in both RNA-seq perturbation data sets (Fig. 6b). Therefore, genes bound by NFIX and showing expression changes in both datasets where NFIX was perturbed, albeit using different approaches, were considered to be high-confidence target genes of NFIX.

Ultimately, this focussed, multifaceted approach led us to identify 90 potential NFIX target genes. While we focussed here on *Itsn1*, the role of NFIX in mediating other genes identified via this screen offers a number of interesting avenues of future research. For example, the factors mediating the transcriptional activation of the *Nfis* themselves is very poorly defined. Our findings suggest that NFIX may autoregulate

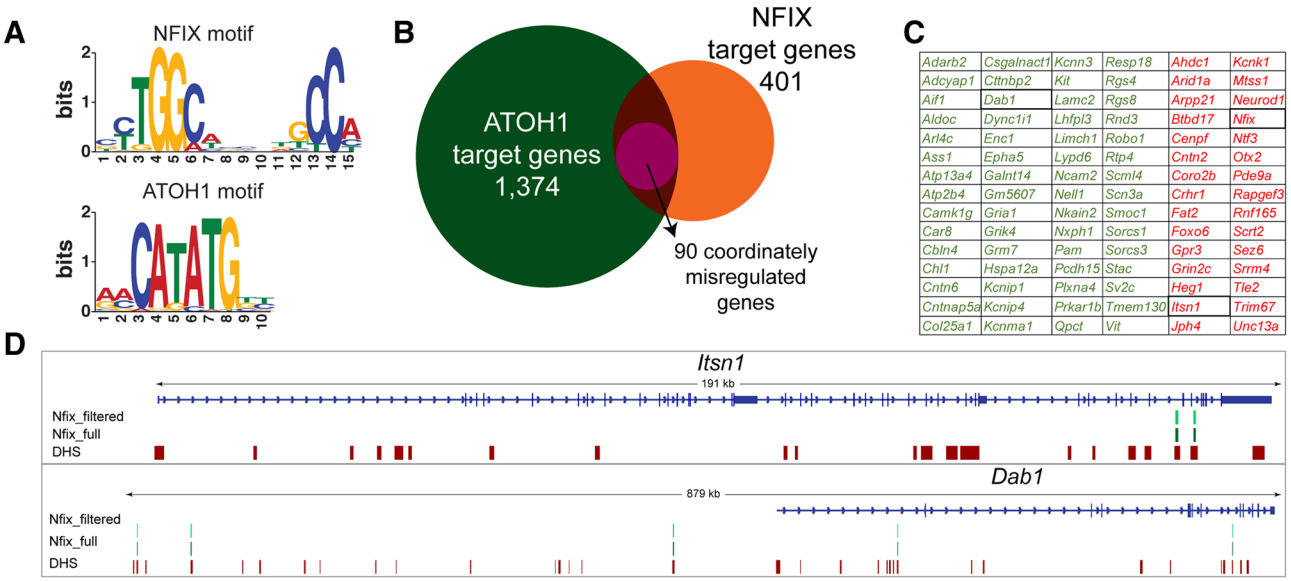

Fig. 6 Combined analysis of *Nfix*$^{-/-}$ GNPs and *Atoh1*$^{-/-}$ cerebellar tissue. **a** MEME-suite de novo motif discovery run on NFIX ChIP-seq peaks revealed both the NFI motif, and the ATOH1 motif, suggesting the two transcription factors potentially regulate a common suite of target genes. **b** Comparison of 1551 genes bound by ATOH1 and misregulated in *Atoh1*$^{-/-}$ cerebellar tissue (Klisch et al. 2011) and 578 genes bound by NFIX and misregulated in *Nfix*$^{-/-}$ GNPs identified 177 shared target genes. Of the 177 shared target genes, 90 were coordinately misregulated (i.e. up in both datasets, or down in both datasets) in both *Atoh1*$^{-/-}$ cerebellar tissue (Klisch et al. 2011) and *Nfix*$^{-/-}$ GNPs. These 90 genes are listed in **c**, with those genes in red being downregulated in *Nfix*$^{-/-}$ GNPs, and those genes in green being upregulated in *Nfix*$^{-/-}$ GNPs. The remaining 87 genes were not coordinately misregulated in the two datasets (i.e. expression was up in one dataset and down in the other, or *vice versa*). **d** Shows genome browser tracks for the regions around the *Itsn1* and *Dab1* genes. The tracks reveal NFIX binding sites from our ChIP-seq dataset (NFIX_full, dark green), NFIX binding sites that appear in regions of accessible chromatin (NFIX_filtered, light green) and regions of open chromatin from published DNase 1 hypersensitivity analysis (DHS, red). *Itsn1* has binding events occurring intronically and *Dab1* has binding events occurring distally and intronically

itself, a finding consistent with a recent report identifying NFIB as a regulator of *Nfix* expression in the developing spinal cord (Matuzelski et al. 2017). Moreover, investigating the expression and role of other novel factors highlighted in this screen will enhance our understanding of GNP biology. Another point to consider is the fact that we filtered our target gene list (RNA-seq and ChIP-seq; Fig. 5d) following our use of motif enrichment, which identified the ATOH1 consensus binding site within our NFIX ChIP-seq peaks (Fig. 6a, b). We filtered our gene list based on those genes that were also potential targets of ATOH1 [i.e. contained an ATOH1 ChIP-seq peak, and were differentially regulated in *Atoh1*-deficient cerebellar tissue (Klisch et al. 2011)]. Many potential NFIX target genes (401 in total) were not identified in the ATOH1 datasets, and as such, many more avenues remain to study novel targets of NFIX in GNP differentiation (e.g. *Tiam2, Lingo3, Adamts1*). Finally, we also filtered our NFIX ChIP-seq peaks by only considering those peaks located within open chromatin (Frank et al. 2015). An interesting finding of our ChIP-seq data was that many of the peaks were located in regions of closed chromatin. This suggests that NFIX may play roles in addition to regulating direct gene transcription. Indeed, NFIs have previously been shown to bind to histone H3, and to regulate nucleosomal architecture (Fane et al. 2017; Esnault et al. 2009; Muller and Mermod 2000). NFIB was also shown recently to regulate chromatin accessibility in small cell lung cancer in a manner that promoted tumour metastasis (Denny et al. 2016). Looking forward, defining the functional significance of NFIX binding to closed regions of chromatin may provide new insights into how these factors regulate neural stem cell biology.

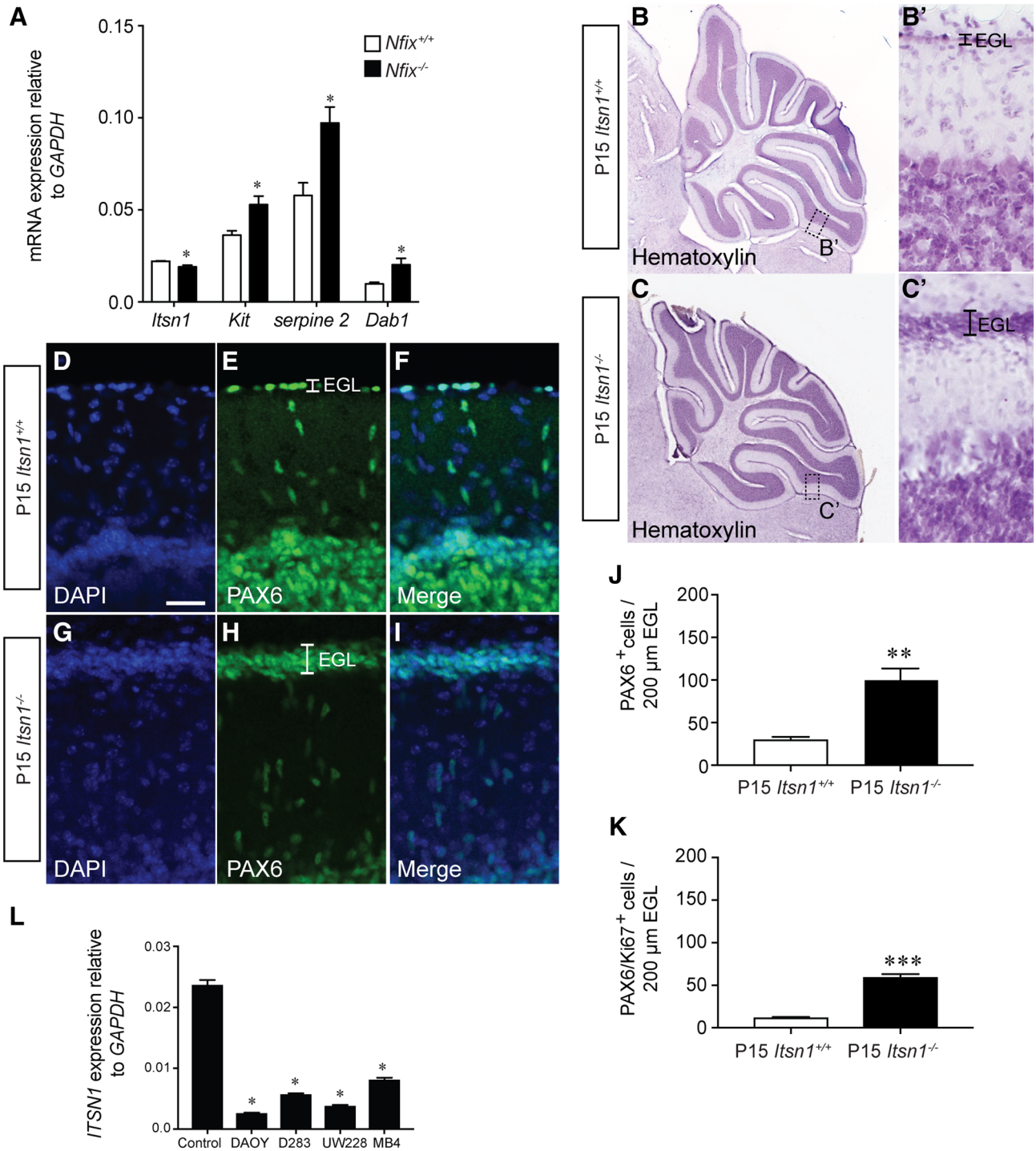

Fig. 7 *Intersectin 1* is a downstream target for NFIX in GNP development. **a** qPCR performed on P7 GNPs from wild-type and $Nfix^{-/-}$ mice revealed significantly reduced levels of *Itsn1*. Levels of *Kit, serpine 2* and *Dab1* were, conversely, significantly elevated in the mutant in comparison to the controls. **b, c** Mid-sagittal sections of P15 wild-type (**b**) and $Itsn1^{-/-}$ (**c**) mice stained with hematoxylin. Gross morphology of the cerebellum was not altered in the absence of *Itsn1*. The boxed regions in **b** and **c** are shown in **b'** and **c'**, respectively. These reveal that the EGL is markedly larger in $Itsn1^{-/-}$ mice on comparison to the controls. **d–i** Immunofluorescence staining with PAX6 revealed that, whereas few PAX6-expressing cells remained in the EGL of wild-type mice (**d–f**) at this age, there were numerous PAX6-expressing GNPs in the EGL of $Itsn1^{-/-}$ mice (**g–i**). Quantitation of the EGL of P15 mice revealed significantly more PAX6-expressing (**j**) and PAX6/Ki67-expressing (**k**) cells in the EGL of the mutant in comparison to the control at P15. **l** qPCR revealed that different medulloblastoma cell lines had significantly lower *ITSN1* expression in comparison to normal cerebellar tissue. $*p<0.05$, $**p<0.01$, $***p<0.001$ *t* test

Acknowledgements This work was supported by a Cancer Council Queensland Grant (MP), an Australian Research Council grants (DP160100368, DP180100017 to MP) and NYSTEM grants (CO30133 and C30290GG to RMG). MP was supported by a fellowship (Australian Research Council Future Fellowship; FT120100170). JF and AE were supported by Australian Postgraduate Awards. ASB was supported by Ruth L. Kirschstein NRSA F32 GM105227.

Compliance with ethical standards

Conflict of interest The authors declare that they have no conflict of interest.

References

Adams A, Thorn JM, Yamabhai M, Kay BK, O'Bryan JP (2000) Intersectin, an adaptor protein involved in clathrin-mediated endocytosis, activates mitogenic signaling pathways. JBC 275(35):27414–27420

Aruga J (2004) The role of Zic genes in neural development. Mol Cell Neurosci 26(2):205–221

Aruga J, Inoue T, Hoshino J, Mikoshiba K (2002) Zic2 controls cerebellar development in cooperation with Zic1. J Neurosci 22(1):218–225

Bailey TL, Boden M, Buske FA, Frith M, Grant CE, Clementi L, Ren J, Li WW, Noble WS (2009) MEME SUITE: tools for motif discovery and searching. Nucleic Acids Res 37:W202–W208 (**Web Server issue**)

Blythe SA, Reid CD, Kessler DS, Klein PS (2009) Chromatin immunoprecipitation in early *Xenopus laevis* embryos. Dev Dyn 238(6):1422–1432

Campbell CE, Piper M, Plachez C, Yeh YT, Baizer JS, Osinski JM, Litwack ED, Richards LJ, Gronostajski RM (2008) The transcription factor Nfix is essential for normal brain development. BMC Dev Biol 8:52

Cavalli FMG, Remke M, Rampasek L, Peacock J, Shih DJH, Luu B, Garzia L, Torchia J, Nor C, Morrissy AS, Agnihotri S, Thompson YY, Kuzan-Fischer CM, Farooq H, Isaev K, Daniels C, Cho BK, Kim SK, Wang KC, Lee JY, Grajkowska WA, Perek-Polnik M, Vasiljevic A, Faure-Conter C, Jouvet A, Giannini C, Nageswara Rao AA, Li KKW, Ng HK, Eberhart CG, Pollack IF, Hamilton RL, Gillespie GY, Olson JM, Leary S, Weiss WA, Lach B, Chambless LB, Thompson RC, Cooper MK, Vibhakar R, Hauser P, van Veelen MC, Kros JM, French PJ, Ra YS, Kumabe T, Lopez-Aguilar E, Zitterbart K, Sterba J, Finocchiaro G, Massimino M, Van Meir EG, Osuka S, Shofuda T, Klekner A, Zollo M, Leonard JR, Rubin JB, Jabado N, Albrecht S, Mora J, Van Meter TE, Jung S, Moore AS, Hallahan AR, Chan JA, Tirapelli DPC, Carlotti CG, Fouladi M, Pimentel J, Faria CC, Saad AG, Massimi L, Liau LM, Wheeler H, Nakamura H, Elbabaa SK, Perezpena-Diazconti M, Chico Ponce de Leon F, Robinson S, Zapotocky M, Lassaletta A, Huang A, Hawkins CE, Tabori U, Bouffet E, Bartels U, Dirks PB, Rutka JT, Bader GD, Reimand J, Goldenberg A, Ramaswamy V, Taylor MD (2017) Intertumoral heterogeneity within medulloblastoma subgroups. Cancer Cell 31(6):737–754.e736

Chang CY, Pasolli HA, Giannopoulou EG, Guasch G, Gronostajski RM, Elemento O, Fuchs E (2013) NFIB is a governor of epithelial-melanocyte stem cell behaviour in a shared niche. Nature 495(7439):98–102

Chaudhry AZ, Lyons GE, Gronostajski RM (1997) Expression patterns of the four nuclear factor I genes during mouse embryogenesis indicate a potential role in development. Dev Dyn 208(3):313–325

Chen KS, Harris L, Lim JWC, Harvey TJ, Piper M, Gronostajski RM, Richards LJ, Bunt J (2017) Differential neuronal and glial expression of nuclear factor I proteins in the cerebral cortex of adult mice. J Comp Neurol 525(11):2465–2483

Chizhikov V, Millen KJ (2003) Development and malformations of the cerebellum in mice. Mol Genet Metab 80(1–2):54–65

Deneen B, Ho R, Lukaszewicz A, Hochstim CJ, Gronostajski RM, Anderson DJ (2006) The transcription factor NFIA controls the onset of gliogenesis in the developing spinal cord. Neuron 52(6):953–968

Denny SK, Yang D, Chuang CH, Brady JJ, Lim JS, Gruner BM, Chiou SH, Schep AN, Baral J, Hamard C, Antoine M, Wislez M, Kong CS, Connolly AJ, Park KS, Sage J, Greenleaf WJ, Winslow MM (2016) Nfib promotes metastasis through a widespread increase in chromatin accessibility. Cell 166(2):328–342

Dixon C, Harvey TJ, Smith AG, Gronostajski RM, Bailey TL, Piper M (2013) Nuclear factor one X Regulates bobby sox during development of the mouse forebrain. Cell Mol Neurobiol 33:867–873

Engelkamp D, Rashbass P, Seawright A, van Heyningen V (1999) Role of Pax6 in development of the cerebellar system. Development 126(16):3585–3596

Esnault G, Majocchi S, Martinet D, Besuchet-Schmutz N, Beckmann JS, Mermod N (2009) Transcription factor CTF1 acts as a chromatin domain boundary that shields human telomeric genes from silencing. Mol Cell Biol 29(9):2409–2418

Fane M, Harris L, Smith AG, Piper M (2017) Nuclear factor one transcription factors as epigenetic regulators in cancer. Int J Cancer 140(12):2634–2641

Feng J, Liu T, Qin B, Zhang Y, Liu XS (2012) Identifying ChIP-seq enrichment using MACS. Nat Protoc 7(9):1728–1740

Frank CL, Liu F, Wijayatunge R, Song L, Biegler MT, Yang MG, Vockley CM, Safi A, Gersbach CA, Crawford GE, West AE (2015) Regulation of chromatin accessibility and Zic binding at enhancers in the developing cerebellum. Nat Neurosci 18(5):647–656

Fraser J, Essebier A, Gronostajski RM, Boden M, Wainwright BJ, Harvey TJ, Piper M (2017) Cell-type-specific expression of NFIX in the developing and adult cerebellum. Brain Struct Funct 222(5):2251–2270

Gallagher E, Howell BW, Soriano P, Cooper JA, Hawkes R (1998) Cerebellar abnormalities in the disabled (mdab1-1) mouse. J Comp Neurol 402(2):238–251

Genovesi LA, Ng CG, Davis MJ, Remke M, Taylor MD, Adams DJ, Rust AG, Ward JM, Ban KH, Jenkins NA, Copeland NG, Wainwright BJ (2013) Sleeping Beauty mutagenesis in a mouse medulloblastoma model defines networks that discriminate between human molecular subgroups. Proc Natl Acad Sci USA 110(46):E4325–E4334

Gubar O, Morderer D, Tsyba L, Croise P, Houy S, Ory S, Gasman S, Rynditch A (2013) Intersectin: the crossroad between vesicle exocytosis and endocytosis. Front Endocrinol 4:109

Guertin MJ, Lis JT (2013) Mechanisms by which transcription factors gain access to target sequence elements in chromatin. Curr Opin Genet Dev 23(2):116–123

Harris L, Genovesi LA, Gronostajski RM, Wainwright BJ, Piper M (2015) Nuclear factor one transcription factors: divergent functions in developmental versus adult stem cell populations. Dev Dyn 244(3):227–238

Harris L, Zalucki O, Gobius I, McDonald H, Osinki J, Harvey TJ, Essebier A, Vidovic D, Gladwyn-Ng I, Burne TH, Heng JI, Richards LJ, Gronostajski RM, Piper M (2016) Transcriptional regulation of intermediate progenitor cell generation during hippocampal development. Development 143(24):4620–4630

Harris L, Zalucki O, Clement O, Fraser J, Matuzelski E, Oishi S, Harvey TJ, Burne THJ, Heng JI, Gronostajski RM, Piper M (2018) Neurogenic differentiation by hippocampal neural stem

and progenitor cells is biased by NFIX expression. Development. https://doi.org/10.1242/dev.155689
Heng YH, Barry G, Richards LJ, Piper M (2012) Nuclear factor I genes regulate neuronal migration. Neuro-Signals 20(3):159–167
Heng YH, McLeay RC, Harvey TJ, Smith AG, Barry G, Cato K, Plachez C, Little E, Mason S, Dixon C, Gronostajski RM, Bailey TL, Richards LJ, Piper M (2014) NFIX regulates neural progenitor cell differentiation during hippocampal morphogenesis. Cereb Cortex 24(1):261–279
Heng YH, Zhou B, Harris L, Harvey T, Smith A, Horne E, Martynoga B, Andersen J, Achimastou A, Cato K, Richards LJ, Gronostajski RM, Yeo GS, Guillemot F, Bailey TL, Piper M (2015) NFIX regulates proliferation and migration within the murine SVZ neurogenic niche. Cereb Cortex 25(10):3758–3778
Herrero-Garcia E, O'Bryan JP (2017) Intersectin scaffold proteins and their role in cell signaling and endocytosis. Biochim Biophys Acta 1864(1):23–30
Huang da W, Sherman BT, Lempicki RA (2009a) Bioinformatics enrichment tools: paths toward the comprehensive functional analysis of large gene lists. Nucleic Acids Res 37(1):1–13
Huang da W, Sherman BT, Lempicki RA (2009b) Systematic and integrative analysis of large gene lists using DAVID bioinformatics resources. Nat Protoc 4(1):44–57
Hughes TR (2011) Introduction to "a handbook of transcription factors". Subcell Biochem 52:1–6
Jakob B, Kochlamazashvili G, Japel M, Gauhar A, Bock HH, Maritzen T, Haucke V (2017) Intersectin 1 is a component of the Reelin pathway to regulate neuronal migration and synaptic plasticity in the hippocampus. Proc Natl Acad Sci U S A 114(21):5533–5538
Kang P, Lee HK, Glasgow SM, Finley M, Donti T, Gaber ZB, Graham BH, Foster AE, Novitch BG, Gronostajski RM, Deneen B (2012) Sox9 and NFIA coordinate a transcriptional regulatory cascade during the initiation of gliogenesis. Neuron 74(1):79–94
Kawauchi D, Saito T (2008) Transcriptional cascade from Math1 to Mbh1 and Mbh2 is required for cerebellar granule cell differentiation. Dev Biol 322(2):345–354
Kilpatrick DL, Wang W, Gronostajski R, Litwack ED (2012) Nuclear factor I and cerebellar granule neuron development: an intrinsic-extrinsic interplay. Cerebellum 11(1):41–49
Klaassens M, Morrogh D, Rosser EM, Jaffer F, Vreeburg M, Bok LA, Segboer T, van Belzen M, Quinlivan RM, Kumar A, Hurst JA, Scott RH (2015) Malan syndrome: Sotos-like overgrowth with de novo NFIX sequence variants and deletions in six new patients and a review of the literature. Eur J Hum Genet 23(5):610–615
Klisch TJ, Xi Y, Flora A, Wang L, Li W, Zoghbi HY (2011) In vivo Atoh1 targetome reveals how a proneural transcription factor regulates cerebellar development. Proc Natl Acad Sci USA 108(8):3288–3293
Kumbasar A, Plachez C, Gronostajski RM, Richards LJ, Litwack ED (2009) Absence of the transcription factor Nfib delays the formation of the basilar pontine and other mossy fiber nuclei. J Comp Neurol 513(1):98–112
Landsberg RL, Awatramani RB, Hunter NL, Farago AF, DiPietrantonio HJ, Rodriguez CI, Dymecki SM (2005) Hindbrain rhombic lip is comprised of discrete progenitor cell populations allocated by Pax6. Neuron 48(6):933–947
Langmead B, Salzberg SL (2012) Fast gapped-read alignment with Bowtie 2. Nat Methods 9(4):357–359
Lee HY, Greene LA, Mason CA, Manzini MC (2009) Isolation and culture of post-natal mouse cerebellar granule neuron progenitor cells and neurons. J Vis Exp. https://doi.org/10.3791/990
Leto K, Arancillo M, Becker EB, Buffo A, Chiang C, Ding B, Dobyns WB, Dusart I, Haldipur P, Hatten ME, Hoshino M, Joyner AL, Kano M, Kilpatrick DL, Koibuchi N, Marino S, Martinez S, Millen KJ, Millner TO, Miyata T, Parmigiani E, Schilling K, Sekerkova G, Sillitoe RV, Sotelo C, Uesaka N, Wefers A, Wingate RJ, Hawkes R (2015) Consensus paper: cerebellar development. Cerebellum 15(6):789–828
Machanick P, Bailey TL (2011) MEME-ChIP: motif analysis of large DNA datasets. Bioinformatics 27(12):1696–1697
Machold R, Fishell G (2005) Math1 is expressed in temporally discrete pools of cerebellar rhombic-lip neural progenitors. Neuron 48(1):17–24
Malan V, Rajan D, Thomas S, Shaw AC, Louis Dit Picard H, Layet V, Till M, van Haeringen A, Mortier G, Nampoothiri S, Puseljic S, Legeai-Mallet L, Carter NP, Vekemans M, Munnich A, Hennekam RC, Colleaux L, Cormier-Daire V (2010) Distinct effects of allelic NFIX mutations on nonsense-mediated mRNA decay engender either a Sotos-like or a Marshall-Smith syndrome. Am J Hum Genet 87(2):189–198
Martinez S, Andreu A, Mecklenburg N, Echevarria D (2013) Cellular and molecular basis of cerebellar development. Front Neuroanat 7:18
Matuzelski E, Bunt J, Harkins D, Lim JWC, Gronostajski RM, Richards LJ, Harris L, Piper M (2017) Transcriptional regulation of Nfix by NFIB drives astrocytic maturation within the developing spinal cord. Dev Biol 432(2):286–297
Messina G, Biressi S, Monteverde S, Magli A, Cassano M, Perani L, Roncaglia E, Tagliafico E, Starnes L, Campbell CE, Grossi M, Goldhamer DJ, Gronostajski RM, Cossu G (2010) Nfix regulates fetal-specific transcription in developing skeletal muscle. Cell 140(4):554–566
Miale IL, Sidman RL (1961) An autoradiographic analysis of histogenesis in the mouse cerebellum. Exp Neurol 4:277–296
Muller K, Mermod N (2000) The histone-interacting domain of nuclear factor I activates simian virus 40 DNA replication in vivo. JBC 275(3):1645–1650
O'Connor T, Boden M, Bailey TL (2017) CisMapper: predicting regulatory interactions from transcription factor ChIP-seq data. Nucleic Acids Res 45(4):e19
Pan N, Jahan I, Lee JE, Fritzsch B (2009) Defects in the cerebella of conditional Neurod1 null mice correlate with effective Tg(Atoh1-cre) recombination and granule cell requirements for Neurod1 for differentiation. Cell Tissue Res 337(3):407–428
Piper M, Moldrich RX, Lindwall C, Little E, Barry G, Mason S, Sunn N, Kurniawan ND, Gronostajski RM, Richards LJ (2009) Multiple non-cell-autonomous defects underlie neocortical callosal dysgenesis in Nfib-deficient mice. Neural Dev 4(1):43
Piper M, Barry G, Hawkins J, Mason S, Lindwall C, Little E, Sarkar A, Smith AG, Moldrich RX, Boyle GM, Tole S, Gronostajski RM, Bailey TL, Richards LJ (2010) NFIA controls telencephalic progenitor cell differentiation through repression of the Notch effector Hes1. J Neurosci 30(27):9127–9139
Piper M, Harris L, Barry G, Heng YH, Plachez C, Gronostajski RM, Richards LJ (2011) Nuclear factor one X regulates the development of multiple cellular populations in the postnatal cerebellum. J Comp Neurol 519(17):3532–3548
Piper M, Barry G, Harvey TJ, McLeay R, Smith AG, Harris L, Mason S, Stringer BW, Day BW, Wray NR, Gronostajski RM, Bailey TL, Boyd AW, Richards LJ (2014) NFIB-mediated repression of the epigenetic factor Ezh2 regulates cortical development. J Neurosci 34(8):2921–2930
Ransohoff KJ, Tang JY, Sarin KY (2015) Squamous change in basal-cell carcinoma with drug resistance. N Engl J Med 373(11):1079–1082
Roussel MF, Hatten ME (2011) Cerebellum development and medulloblastoma. Curr Top Dev Biol 94:235–282
Sanchez-Ortiz E, Cho W, Nazarenko I, Mo W, Chen J, Parada LF (2014) NF1 regulation of RAS/ERK signaling is required for

appropriate granule neuron progenitor expansion and migration in cerebellar development. Genes Dev 28(21):2407–2420

Sengar AS, Ellegood J, Yiu AP, Wang H, Wang W, Juneja SC, Lerch JP, Josselyn SA, Henkelman RM, Salter MW, Egan SE (2013) Vertebrate intersectin1 is repurposed to facilitate cortical midline connectivity and higher order cognition. J Neurosci 33(9):4055–4065

Shu T, Butz KG, Plachez C, Gronostajski RM, Richards LJ (2003) Abnormal development of forebrain midline glia and commissural projections in Nfia knock-out mice. J Neurosci 23(1):203–212

Tamada A, Kumada T, Zhu Y, Matsumoto T, Hatanaka Y, Muguruma K, Chen Z, Tanabe Y, Torigoe M, Yamauchi K, Oyama H, Nishida K, Murakami F (2008) Crucial roles of Robo proteins in midline crossing of cerebellofugal axons and lack of their up-regulation after midline crossing. Neural Dev 3:29

Trapnell C, Roberts A, Goff L, Pertea G, Kim D, Kelley DR, Pimentel H, Salzberg SL, Rinn JL, Pachter L (2012) Differential gene and transcript expression analysis of RNA-seq experiments with TopHat and Cufflinks. Nat Protoc 7(3):562–578

Vaswani AR, Blaess S (2016) Reelin signaling in the migration of ventral brain stem and spinal cord neurons. Front Cell Neurosci 10:62

Vernay B, Koch M, Vaccarino F, Briscoe J, Simeone A, Kageyama R, Ang SL (2005) Otx2 regulates subtype specification and neurogenesis in the midbrain. J Neurosci 25(19):4856–4867

Vidovic D, Davila RA, Gronostajski RM, Harvey TJ, Piper M (2018) Transcriptional regulation of ependymal cell maturation within the postnatal brain. Neural Dev 13(1):2

Wang W, Stock RE, Gronostajski RM, Wong YW, Schachner M, Kilpatrick DL (2004) A role for nuclear factor I in the intrinsic control of cerebellar granule neuron gene expression. JBC 279(51):53491–53497

Wang W, Mullikin-Kilpatrick D, Crandall JE, Gronostajski RM, Litwack ED, Kilpatrick DL (2007) Nuclear factor I coordinates multiple phases of cerebellar granule cell development via regulation of cell adhesion molecules. J Neurosci 27(23):6115–6127

Wang W, Crandall JE, Litwack ED, Gronostajski RM, Kilpatrick DL (2010) Targets of the nuclear factor I regulon involved in early and late development of postmitotic cerebellar granule neurons. J Neurosci Res 88(2):258–265

Yue S, Tang LY, Tang Y, Tang Y, Shen QH, Ding J, Chen Y, Zhang Z, Yu TT, Zhang YE, Cheng SY (2014) Requirement of Smurf-mediated endocytosis of Patched1 in sonic hedgehog signal reception. Elife. https://doi.org/10.7554/eLife.02555

Zhao X, Ponomaryov T, Ornell KJ, Zhou P, Dabral SK, Pak E, Li W, Atwood SX, Whitson RJ, Chang AL, Li J, Oro AE, Chan JA, Kelleher JF, Segal RA (2015) RAS/MAPK activation drives resistance to Smo inhibition, metastasis, and tumor evolution in shh pathway-dependent tumors. Cancer Res 75(17):3623–3635